High-efficiency LED COB device combined diced V-shaped pattern and remote phosphor

Zongtao Li (李宗涛)[1], Huiyu Wang (王卉玉)[1], Binhai Yu (余彬海)[1,*], Xinrui Ding (丁鑫锐)[2], and Yong Tang (汤 勇)[1]

[1]*The Key Laboratory of Surface Functional Structure Manufacturing of Guangdong High Education Institutes, South China University of Technology, Guangzhou 510641, China*

[2]*The Department of Mechanical Engineering, University of California at Berkeley, Berkeley, California 94720-5800, USA*

**Corresponding author: bhaiyu@yeah.net*

Received August 11, 2016; accepted December 28, 2016; posted online January 22, 2017

To further improve the luminous efficiency of LED lightings, this Letter proposes a chip-on-board (COB) device by combining diced staggered V-shaped patterns and remote phosphors. The results show that the V-shaped patterned COB (V-COB) with vertex angles from 120° to 150° can achieve a ~17% output power increase (OPI) compared to the conventional COB. V-COB remote phosphor devices (RPDs) are then manufactured and tested. The luminous efficiency of the proposed RPD represents an 11.6% increase at the correlated color temperature of ~3000 K. Such an improvement can be attributed to both the decreases of total internal reflections and phosphor backscatterings.

OCIS codes: 230.3670, 220.0220, 250.5230.

doi: 10.3788/COL201715.042301.

Phosphor-converted white-light LED devices, insofar as they are used for general lightings[1], backlights[2], and wireless communications[3], can be categorized into those with discrete components and those with chip-on-board (COB) devices. The former are typically comprised of a lead frame, an LED chip, and an optical encapsulant. In practice, multiple discrete LEDs (using a surface-mounting assembly) are required for gaining sufficient luminous flux, which tends to be high cost, forms a multishadow pattern in the illumination area[4,5], and makes the human eyes feel tired. By way of contrast, COBs are able to offer a bright lighting environment, though they utilize only one source. In effect, this allows engineers to easily design high-performance illumination systems with a low cost and without the multishadow pattern.

In a conventional COB, a silicone or phosphor-silicone mixture is directly dispensed to the LED-chip-array for blue-light transmission and downconversion, resulting in a flat encapsulant surface. Light emitted from the chips or the phosphor particles undergoes total internal reflections (TIRs) since the critical angle on the silicone-air interface is only 38° to 45° (refractive index of the silicone is 1.4 to 1.6)[6]. Techniques such as dome-shaped lenses[7], textured silicones[8,9], and TiO_2 encapsulations[10] were proposed to improve the COB light outcoupling. For the first method, the volume of the lens has been improved to ~18000 mm^3, which was 17 times higher than that of the original structure, and made it high cost and difficult to fabricate. In the textured silicone case, a special and unique mold was required for one COB size, and it was against the increasing requirements of product diversity. Introducing of scattering TiO_2 material was an easy way to gain high light-extraction efficiency; however, the setting phenomenon of the exotic particles was rather complex[11,12], which would significantly affect the product consistency. Therefore, these methods were still lacking a practical application. In the recently released CREE flip chip DA1000, the brilliant engineer utilized a V-shaped pattern to cover the surface of the LED chip, and achieved a >60% electro-optical efficiency[13]. This technique was quite impressive to the LED researchers because the pattern was manufactured by a dicing saw, and it was flexible to be adapted to different types of optical microstructures with a high efficiency and low cost[14]. The LED COB and the CREE chip faced the same problem: how to improve the light extraction in a high refractive index difference interface. Both the lecture and the industry are now curious about whether this technique is effective in the former case (LED COBs).

Moreover, the contiguity configuration in the conventional COBs (the chip and the phosphor) would simultaneously backscatter about 60% of the luminous flux to the chips, leading to a large portion of energy absorption[15]. The existing methods only focused on the COB TIR problems, and never considered the backscattering energy loss. Therefore, the efforts to increase the luminous flux were significantly diminished as the phosphor concentration increased[10,16]. This made it a great challenge to fabricate high efficiency COBs with a low correlated color temperature (CCT). Placing the phosphor layer a certain distance away from the chip therefore constituted a better option[17–19], which was referred to as remote phosphor devices (RPDs). This structure reduced the probability of the phosphorescence directly hitting the chip and increased the luminous efficiency[20].

In this Letter, both the diced V-shaped patterns and the remote phosphor are combined to increase the luminous efficiency of low CCT LED COBs. The ray dynamics of

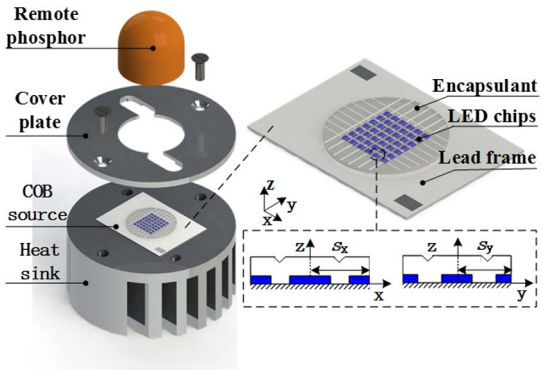

Fig. 1. Schematic diagram of the patterned COB RPD.

the new structure are analyzed for parameter optimization. Both the conventional and the V-shaped patterned COB (V-COB) RPDs are then manufactured and tested.

The V-COB RPD consisted of a dome-shaped remote phosphor, a patterned COB, a heat sink, and a cover plate, as shown in Fig. 1. In order to improve the luminous efficiency of the COB RPDs, a staggered V-shaped pattern was used on the surface of the COB encapsulant; the remote phosphor composed of YAG:Ce and nitride materials entirely covered the luminous area in order to make full use of the blue wavelength downconversion and produce white light. The radius and height of the remote phosphor were 8.5 and 14.5 mm, respectively.

We first optimized the staggered V-shaped pattern on the COB encapsulant by using the commercial software Tracepro. The simulation schematic diagram of the V-COB is shown in Fig. 1. The size of the chip was 0.76 mm × 0.56 mm, the intervals along the x and y axes were 1.1 and 1 mm, respectively; the height of the silicone encapsulant was 0.5 mm; and the refractive index was 1.54. The staggered V-shaped pattern was centered between chips with a depth of 0.1 mm and a vertex angle of 15° to 165° (with a step of 5°). The emitted light from the chips took on a Lambertian distribution with a wavelength of 450 nm. The reflectivity of the lead frame was 95%.

Figure 2 shows the output power increase (OPI) of the V-COBs, which were divided into 4 stages. In stage A (angles from 15° to 75°), the OPI increases rapidly. That is because, as the vertex angle increases in this range, rays (emitting angles larger than the encapsulant critical escape angle of 40° for a refractive index of 1.54) will probably propagate to the walls of the V-shaped pattern and escape from the encapsulant. Figure 3(a) shows the typical ray dynamics of these situations. In stage B (angles from 75° to 105°), the OPI slightly decreases as the vertex angle increases. Under these conditions, rays that escape from the encapsulant would probably be re-captured by the silicone, as shown in Fig. 3(b). At stage C (angles from 105° to 135°), the OPI exhibits a second increase. In this case, most of the space between the chips has been covered by the V-shaped pattern, and more rays will propagate to the side walls. In addition, it can be found that rays in the

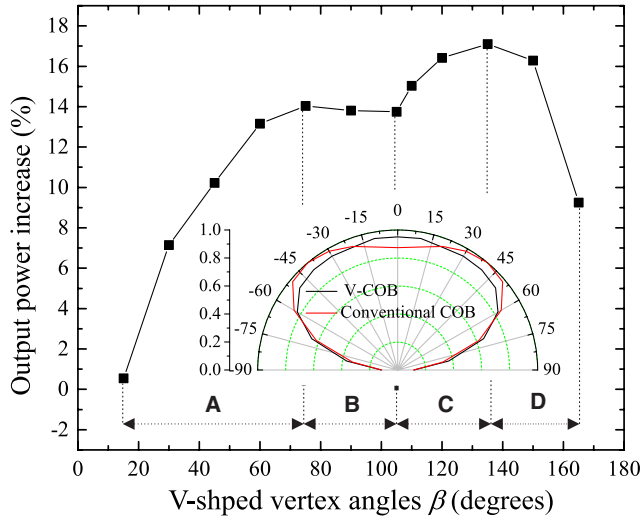

Fig. 2. Simulated OPI of a patterned COB with different V-shaped vertex angles, compared with that of a conventional COB. The inset shows the angular intensity distribution of the COB with a vertex angle of 120° as well as that of the conventional COB.

small emitting angle range will propagate to the encapsulant surface with smaller incident angles, as shown in Fig. 3(c). At stage D (angles from 135° to 165°), the enlarged vertex angle decreases the OPI sharply and eclipses the advantages of the V-shaped pattern. TIRs become common again to the rays with emitting angles larger than 64°. This is very similar to the situations in conventional COBs. Figure 3(d) reveals the typical ray dynamics, where rays (e.g., rays with emitting angles of 49°) propagate to the pattern side wall and escape for small vertex angles (e.g., 135°). However, they reach the patterns and experience TIR in the case of large vertex angles (e.g., 165°). On the other hand, the V-shaped pattern not only covers the space between chips at this stage, but also covers the front of the chips. For the rays near the normal direction, the

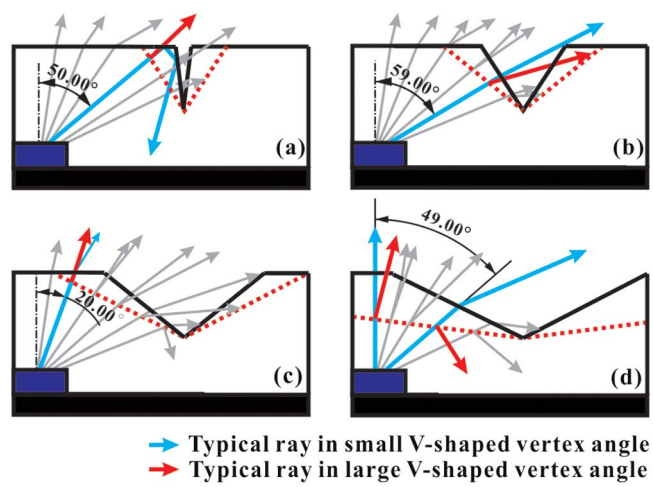

Fig. 3. Schematic diagrams of the ray dynamics for patterned COBs with different V-shaped vertex angles.

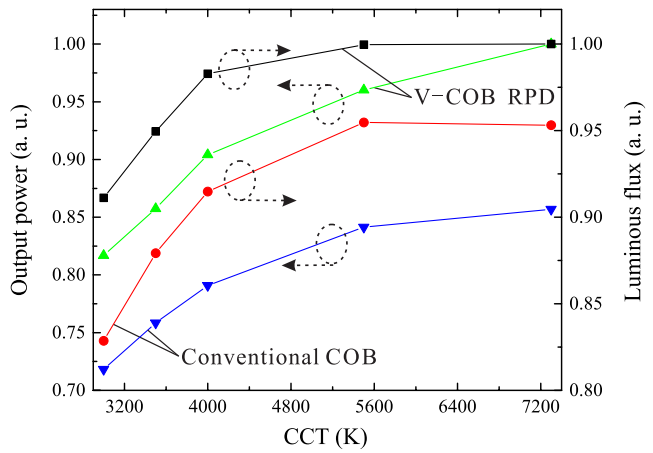

Fig. 4. Simulated output power and luminous flux of the V-COB RPD and conventional COB with different CCTs.

modification of the vertex angle leads to an enhancement of Fresnel loss owing to the increase of ray incident angles.

Generally, the highest OPI of the patterned COBs exhibits a 17.1% improvement compared to the conventional COBs. The optimal vertex angle falls in the range of 120° to 150°.

One of the optimal V-COBs (vertex angle = 120°) was further studied in the RPD simulations through the method presented in our previous study[21]. The results indicate that the output power of the V-COB RPD has been increased by ∼14% at a very large CCT range, as shown in Fig. 4. In this situation, the OPI can be explained by the following factors: 1) the V-shaped pattern leads to significant light-extraction improvement; 2) the concentrated bluelight intensity (inset in Fig. 2) reduces the optical path of rays in the phosphor shell and lowers the backscattering loss. Considered about the sensitivity of human eyes to different spectra, the new RPD releases an ∼10% higher luminous flux at the CCT of 3000 K.

Then, the V-COBs with the vertex angle of 120° were manufactured by Disco DAD322 dicing saw, as shown in Fig. 5(a). A ∅54 mm V-shape pre-formed diamond blade was utilized. The maximum revolution speed of the spindle is 40000 rpm. The depth of the pattern is 100 μm. High pressure deionized water was used for cooling. The whole process can be shortened to ∼20 s, which is much less than for lens molding (the molding process takes about

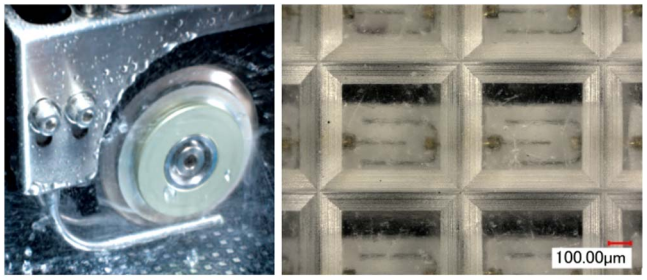

Fig. 5. Manufacturing process of the V-COB by (a) the Disco DAD322 dicing saw and (b) the finished V-shaped pattern.

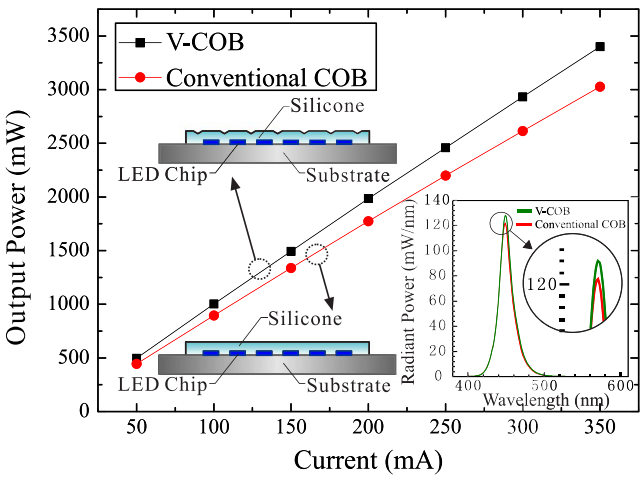

Fig. 6. Measured output power of COBs under different drive currents. The inset shows the spectra of the COBs (350 mA).

500 s per cycle). The finished pattern is shown in Fig. 5(b). For comparison, conventional COBs are also fabricated and tested; the efficiency of the LED chips used in this study remains the same in all devices.

Figure 6 depicts the output power of the COBs. It can be found that the output power of the conventional COB and the V-COB increases linearly. Compared with conventional structures, the output power of V-COBs rises more rapidly; in particular, the increasing rates are 8.6 and 9.7 mW/mA, respectively. Under the typical conditions of a 350 mA drive current, the V-COB emits a total output power of 3400.8 mW, which is 12.3% higher than that of the conventional COB. The inset in Fig. 6 shows the spectra of the COBs (350 mA) from which it can be observed that the peak wavelength (449 nm) remains unshifted. Furthermore, the V-COBs release a peak output power of up to 128.2 mW/nm, which is 6.3 mW/nm higher than that of the conventional COB. The improved light extraction of V-COBs can be explained by the fact that when the staggered V-shaped pattern was utilized in the surface modification of the silicone encapsulant the rays (in the emitting angles larger than encapsulant critical escape angle) that were supposed to be TIRed from the silicone-air interface retain a chance of escaping.

By assembling a dome-shaped phosphor shell (composed of 13.7 wt. % YAG:Ce and 1.7 wt. % nitride materials) to the new COB, a novel white-light RPD was obtained, as shown in Fig. 7. Figure 8 reveals the luminous output in which the CCT is around 3000–3100 K. It can be seen that, owing to the significantly enhanced output power of the V-COB and notable decrease of backscattering energy loss, the new RPD emits a much higher luminous flux. In particular, under the typical drive current of 350 mA, the luminous output of the V-COB RPD is 11.6% higher than that of conventional structures, agreeing well with simulation.

We propose a novel high-efficiency V-COB RPD with a low CCT. We first optimize the V-shaped pattern in modifying the surface of the blue-light source. The results show

Fig. 7. Finished LED COB device combined diced V-shaped pattern and remote phosphor.

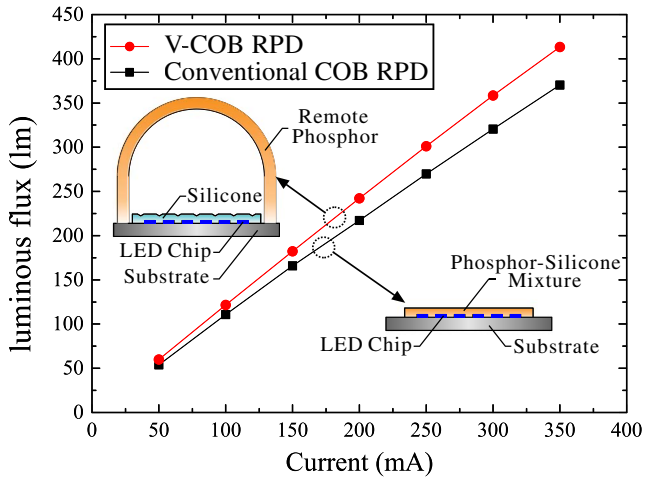

Fig. 8. Measured luminous flux of COB RPDs as a function of drive current.

that the staggered pattern with V-shaped angles from 120° to 150° is able to achieve high OPI values. The highest OPI of the patterned COB is 17.1%, as compared with the conventional COB. These results can be attributed to the fact that the staggered V-shaped pattern is able to reduce the TIR and Fresnel losses. In addition, due to the significant decrease of phosphor backscattering, the V-COB RPD simulations confirm the light extraction efficiency boost with an increase of ~14% at a CCT range from 3000 to ~7000 K. Finally, V-COB RPDs are manufactured by the highly efficient dicing saw technique. The measured results show that the luminous flux of the proposed V-COB RPD increased by 11.6% with the CCT of ~3000 K. We provide a good insight to researchers who are planning to design and fabricate low CCT LED COB devices.

This work was supported by the National Natural Science Foundation of China (Nos. U1401249 and 51375177), the Postdoctoral Science Foundation of China (Nos. 2015T80904 and 2014M560659), and the Fundamental Research Funds for the Central Universities.

References

1. Z.-J. Liu, P. Liu, and F.-H. Yu, Chin. Opt. Lett. **10**, 112201 (2012).
2. Y. Chen, S. Wen, and P. Song, Chin. Opt. Lett. **13**, 032302 (2015).
3. H. Li, Y. Zhang, X. Chen, C. Wu, J. Guo, Z. Gao, and H. Chen, Chin. Opt. Lett. **13**, 080605 (2015).
4. W.-H. Wu, C.-H. Kuo, M.-W. Hung, and K.-C. Huang, Phys. Procedia **19**, 96 (2011).
5. C.-H. Kuo, W.-H. Wu, W.-T. Hsiao, and K.-C. Huang, Phys. Procedia **19**, 233 (2011).
6. Z.-T. Li, Q.-H. Wang, Y. Tang, C. Li, X.-R. Ding, and Z.-H. He, IEEE Trans. Electron. Devices **60**, 1397 (2013).
7. Y. Zhang, J. Xu, M. Ding, D. Zhao, H. Huang, G. Lu, Z. Miao, Y. Qi, B. Zhang, and Y. Cai, IEEE Electron Device Lett. **37**, 197 (2016).
8. X. Luo, R. Hu, S. Liu, and K. Wang, Prog. Energy Combust. Sci. **56**, 1 (2016).
9. H. Xiao, T.-M. Shih, Z.-Q. Guo, Y. Lin, Y.-J. Lu, and Z. Chen, IEEE Trans. Electron Devices **63**, 1128 (2016).
10. H. Zheng, L. Li, X. Lei, X. Yu, S. Liu, and X. Luo, IEEE Electron Device Lett. **35**, 1046 (2014).
11. R. Hu, X. Luo, H. Feng, and S. Liu, J. Lumin. **132**, 1252 (2012).
12. X. Chen, S. Wang, M. Chen, and S. Liu, J. Appl. Polym. Sci. **132**, 42006 (2015).
13. Technical Datasheet, "DA1000 LED chips," [Online]. Available: http://www.cree.com/LED-Chips-and-Materials/Chips/Chips/Direct-Attach/DA1000-LED.
14. M. Maciel, C. Costa, M. Silva, A. Peixoto, R. Wolffenbuttel, and J. Correia, Sens. Actuators A **242**, 210 (2016).
15. N. Narendran, Y. Gu, J. Freyssinier-Nova, and Y. Zhu, Phys. Status Solidi A **202**, R60 (2005).
16. X. Yu, B. Xie, B. Shang, Q. Chen, and X. Luo, IEEE Photon. J. **8**, 1 (2016).
17. S. Yu, Z. Li, G. Liang, Y. Tang, B. Yu, and K. Chen, Photon. Res. **4**, 140 (2016).
18. M.-T. Lin, S.-P. Ying, M.-Y. Lin, K.-Y. Tai, S.-C. Tai, C.-H. Liu, J.-C. Chen, and C.-C. Sun, IEEE Photon. Technol. Lett. **22**, 574 (2010).
19. C.-H. Chiang, H.-Y. Tsai, T.-S. Zhan, H.-Y. Lin, Y.-C. Fang, and S.-Y. Chu, Opt. Lett. **40**, 2830 (2015).
20. E. F. Schubert, J. K. Kim, H. Luo, and J. Xi, Rep. Prog. Phys. **69**, 3069 (2006).
21. J.-S. Li, J.-X. Chen, L.-W. Lin, Z.-T. Li, Y. Tang, B.-H. Yu, and X.-R. Ding, IEEE J. Quantum Electron. **51**, 1 (2015).